Approximate solutions for Forchheimer flow during water injection and water production in an unconfined aquifer

Simon A. Mathias[a,*], Konstantinos N. Moutsopoulos[b]

[a]*Department of Earth Sciences, Durham University, Durham, UK*
[b]*Department of Environmental Engineering, Democritus University of Thrace, Xanthi, Greece*

Abstract

Understanding the hydraulics around injection and production wells in unconfined aquifers associated with rainwater and reclaimed water aquifer storage schemes is an issue of increasing importance. Much work has been done previously to understand the mathematics associated with Darcy's law in this context. However, groundwater flow velocities around injection and production wells are likely to be sufficiently large such as to induce significant non-Darcy effects. This article presents a mathematical analysis to look at Forchheimer's equation in the context of water injection and water production in unconfined aquifers. Three different approximate solutions are derived using quasi-steady-state assumptions and the method of matched asymptotic expansion. The resulting approximate solutions are shown to be accurate for a wide range of practical scenarios by comparison with a finite difference solution to the full problem of concern. The approximate solutions have led to an improved understanding of the flow dynamics of concern. They can also be used as verification tools for future numerical models in this context.

Keywords: Forchheimer equation, Unconfined aquifers, Non-Darcy flow

*Corresponding author. Tel.: +44 (0)1913343491, Fax: +44 (0)1913342301, E-mail address: s.a.mathias@durham.ac.uk

1. Introduction

With the ever increasing significance of climate change induced rainfall variability combined with increasing urban populations, understanding the well hydraulics associated with managed aquifer recharge schemes continues to be an important research topic for water managers around the world (Bouwer, 2002; Dillon, 2005; Sheng, 2005; Pliakas et al., 2005). Such schemes typically involve storing rainwater in aquifers during abundant periods and extracting it when droughts occur (Donovan et al., 2002; Khan, 2008). In some cases, reclaimed wastewater is injected into aquifers with a view that aquifer storage can provide additional treatment (Bouwer, 2002; Dillon, 2005) such that, after sufficient time, the water satisfies local drinking water quality standards (Rygaard et al., 2011).

Appropriate hydraulic models can serve to estimate the conditions under which overflow induced by well recharge might occur (Sheng, 2005), to estimate the recovery potential of stored water, to estimate resident times in aquifers for bioremediation capacity, to forecast negative impacts of recharge on building foundations, pipelines and deep rooted vegetation and to compute energy requirements for aquifer recharge recovery schemes.

In most studies of well hydraulics, it is assumed that the flow behavior can be described by Darcy's law. By further taking into account the continuity equation, the water table evolution in unconfined aquifers can be described by a single non-linear partial differential equation (PDE), the Boussinesq equation (e.g. Bear, 1979).

Existing analytical solutions of the non-linear Boussinesq equation for radial, transient, unconfined flow induced by water injection to an unconfined aquifer are limited to Darcy-flow conditions

and to initially dry aquifer conditions (Yeh and Chang, 2013). Babu and van Genuchten (1980) used similarity transforms to transform the Boussinesq equation to an ordinary differential equation (ODE) and then provided an approximate solution using a perturbation expansion. A similar ODE was derived using similarity transforms by Barenblatt et al. (1990), to which Li et al. (2005) provided asymptotic solutions for both small and large values of the similarity variable. Li et al. (2005) combined these expansions to yield an approximate solution valid for all values of the similarity variable, which they verified by comparison to equivalent numerical results.

Analytical solutions of the linearised radial or two-dimensional Boussinesq equation for transient flow induced by water injection to an unconfined aquifer are more abundant (Hunt, 1971; Marino and Yeh, 1972; Rai and Singh, 1995; Manglik et al., 1997; Teloglou et al., 2008). Both the cases that water is introduced to an aquifer by an injection well (Marino and Yeh, 1972), or by a recharge basin (Rai et al., 1998) are examined. A linearization of the Boussinesq equation either in terms of h, (Rai and Singh, 1995) or in h^2, (where h is the water table elevation relative to the base of the aquifer), is generally adopted. The resulting linear PDE is solved using the Laplace transform method, the finite Hankel transform approach and/or the eigenvalue-eigenfunction method (Marino and Yeh, 1972; Teloglou et al., 2008; Rai et al., 1998). Nevertheless the application range of the solutions above is limited to the case that the perturbation of the water table elevation induced by the water recharge is small.

Due to high velocities, inertial non-Darcy flow conditions may occur in the well vicinity (Mathias and Todman, 2010; Moutsopoulos et al., 2009). Non-Darcy effects cause additional head losses, so that for the injection well problem, the rise of the head at the near well field would be higher than predicted by Darcy's law. The potential engineering implications of these non-Darcy effects

are increased danger of overflow for water injection and increased energy consumption for water production.

Semi-analytical solutions for one-dimensional (non-radial) transient Forcheimer flow in unconfined aquifers have previously been developed by Bordier and Zimmer (2000) and Moutsopoulos (2007, 2009). A semi-analytical solution for one-dimensional steady state radial flow in unconfined aquifers has previously been presented by Terzidis (2003). However, to better understand the role of non-Darcy effects during water injection in unconfined aquifers, we present a series of new approximate analytical solutions to explore one-dimensional transient radial Forchheimer flow in unconfined aquifers.

The outline of this article is as follows: The governing equations for transient one-dimensional radial Forchheimer flow in a homogenous and isotropic unconfined aquifer are presented. The equations are normalized using an appropriate set of dimensionless transformations. Following the ideas of Bordier and Zimmer (2000) and Sen (1986), two different approximate solutions for Darcian flow and strongly non-Darcian flow are derived for initial saturated zones of arbitrary thickness by invoking a quasi-steady-state assumption. Following Mathias et al. (2008), an approximate solution for non-Darcy flow in an aquifer with a moderately deep initial saturated zone is derived using the method of matched asymptotic expansion. The performance of the new approximate solutions are verified by comparison to a finite difference solution of the full problem.

2. Governing equations

Consider the injection/production of water into/from a homogenous and isotropic unconfined aquifer. Considering the so-called Dupuit assumption (that vertical flow is negligible) (Bear,

1979), an appropriate one-dimensional mass conservation equation can be written as

$$S_y \frac{\partial h}{\partial t} = -\frac{1}{r}\frac{\partial (rhq)}{\partial r} \tag{1}$$

where (Forchheimer, 1901)

$$q + \frac{bK}{g}|q|q = -K\frac{\partial h}{\partial r} \tag{2}$$

and S_y [-] is the specific yield, h [L] is the water table elevation above a horizontal impermeable formation, t [T] is time, r [L] is radial distance from an injection well, b [L^{-1}] is the Forchheimer coefficient, K [LT^{-1}] is the hydraulic conductivity of the unconfined aquifer and g [LT^{-2}] is the gravitational acceleration constant.

The relevant initial and boundary conditions can be stated as:

$$\begin{aligned} h &= h_i, && r > 0, && t = 0 \\ 2\pi rhq &= \gamma Q_0, && r \to 0, && t > 0 \\ q &= 0, && r \to \infty, && t > 0 \end{aligned} \tag{3}$$

where h_i [L] is a uniform initial water table elevation, Q_0 [L^3T^{-1}] is a positive valued flow rate associated with a production well or injection well located at $r = 0$ with $\gamma = 1$ for an injection well and $\gamma = -1$ for a production well.

Note that Eq. (2) can rearranged to the form (Mathias et al., 2014; Mathias and Wen, 2015))

$$q = -FK\frac{\partial h}{\partial r} \tag{4}$$

where

$$F = 2\left[1 + \left(1 + \frac{4bK^2}{g}\left|\frac{\partial h}{\partial r}\right|\right)^{1/2}\right]^{-1} \tag{5}$$

3. Dimensionless transformation

It is helpful at this stage to apply the following dimensionless transformations:

$$t_D = \frac{Kt}{S_y H}, \quad r_D = \frac{r}{H}, \quad h_D = \frac{h - h_i}{H}, \quad q_D = \frac{q}{K}, \quad \epsilon = \frac{h_i}{H}, \quad \beta = \frac{bK^2}{g} \tag{6}$$

where

$$H = \left(\frac{Q_0}{2\pi K}\right)^{1/2} \tag{7}$$

such that the above problem reduces to

$$\frac{\partial h_D}{\partial t_D} = -\frac{1}{r_D}\frac{\partial}{\partial r_D}\left[r_D\left(h_D + \epsilon\right)q_D\right] \tag{8}$$

$$q_D = -F\frac{\partial h_D}{\partial r_D} \tag{9}$$

$$F = 2\left[1 + \left(1 + 4\beta\left|\frac{\partial h_D}{\partial r_D}\right|\right)^{1/2}\right]^{-1} \tag{10}$$

$$
\begin{aligned}
&h_D = 0, && r_D > 0, && t_D = 0 \\
&r_D\,(h_D + \epsilon)\,q_D = \gamma, && r_D \to 0, && t_D > 0 \\
&q_D = 0, && r_D \to \infty, && t_D > 0
\end{aligned}
\tag{11}
$$

Note that it is also possible to state that

$$
q_D + \beta |q_D| q_D = -\frac{\partial h_D}{\partial r_D} \tag{12}
$$

4. Analytical solution for large ϵ and zero β

The case of very large ϵ corresponds to the case of very large values of the initial water table elevation or very small values of the flow-rate, such that either the raise in water table elevation induced by water injection or the drawdown induced by water extraction can be assumed negligible. In this way, the cross-sectional area, through which groundwater flow takes place, can be assumed uniform and constant, such that flow processes can be described by the same equations ordinarily used to describe confined aquifers. The case of zero β corresponds to a problem for which the inertial effects are negligible such that the Forchheimer equation reduces to Darcy's law.

For very large ϵ and zero β, the problem reduces to

$$
\frac{\partial h_D}{\partial t_D} = -\frac{\epsilon}{r_D} \frac{\partial (r_D q_D)}{\partial r_D} \tag{13}
$$

$$
\begin{aligned}
h_D &= 0, \qquad r_D > 0, \quad t_D = 0 \\
\epsilon r_D q_D &= \gamma, \quad r_D \to 0, \quad t_D > 0 \\
q_D &= 0, \qquad r_D \to \infty, \quad t_D > 0
\end{aligned}
\tag{14}
$$

$$
q_D = -\frac{\partial h_D}{\partial r_D} \tag{15}
$$

which has the analytical solution (Theis, 1935)

$$
h_D = \frac{\gamma}{2\epsilon} E_1\left(\frac{r_D^2}{4\epsilon t_D}\right) \tag{16}
$$

where E_1 denotes the exponential integral function.

Eq. (16) above is often referred to as the Theis solution and is frequently applied to describe drawdown around a fully penetrating production well situated within a homogenous and isotropic confined aquifer of infinite lateral extent (Bear, 1979).

5. Quasi-steady state solutions

In the following subsections, a series of quasi-steady-state solutions are obtained using a volume balance approach previously applied to obtain an approximate solution for transient non-Darcy radial flow in a confined aquifer by Sen (1986). After some time has passed, the system can be expected to behave as in a quasi-steady-state (Bordier and Zimmer, 2000) such that

$$q_D = \begin{cases} \dfrac{\gamma}{(h_D + \epsilon) r_D}, & 0 \le r_D < r_{eD} \\ \\ 0, & r_D \ge r_{eD} \end{cases} \tag{17}$$

where r_{eD} is a dimensionless radius of influence, which varies with time, t_D. From mass conservation considerations it can be shown that

$$t_D = \gamma \int_0^{r_{eD}} r_D h_D dr_D \tag{18}$$

Noting that

$$h_D = 0, \quad r_D = r_{eD} \tag{19}$$

application of integration by parts to Eq. (18) leads to

$$t_D = \frac{\gamma}{2} \int_0^{h_{0D}} r_D^2 dh_D \tag{20}$$

where

$$h_{0D} = \begin{cases} \infty, & \gamma = 1 \\ \\ -\epsilon, & \gamma = -1 \end{cases} \tag{21}$$

because it is not physically possible for $h_D < -\epsilon$.

5.1. *Approximate solution for zero β*

When $\beta = 0$, Eq. (15) can be substituted into Eq. (17) to yield

$$\frac{\partial h_D}{\partial r_D} = -\frac{\gamma}{(h_D + \epsilon) r_D} \tag{22}$$

Separating variables, integrating both sides of Eq. (22) with respect to r_D and finding the integration constant by imposing Eq. (19) then leads to

$$\frac{h_D^2}{2} + \epsilon h_D = -\gamma \ln\left(\frac{r_D}{r_{eD}}\right) \tag{23}$$

which can be rearranged to obtain

$$h_D = 2\gamma \ln\left(\frac{r_{eD}}{r_D}\right)\left\{\epsilon + \left[\epsilon^2 + 2\gamma \ln\left(\frac{r_{eD}}{r_D}\right)\right]^{1/2}\right\}^{-1} \tag{24}$$

and

$$r_D^2 = r_{eD}^2 \exp\left[-\frac{(h_D^2 + 2\epsilon h_D)}{\gamma}\right] \tag{25}$$

A relationship between r_{eD} and t_D can be obtained by substituting Eq. (25) into Eq. (20) to obtain (Wolfram Research, Inc., 2015)

$$\frac{t_D}{r_{eD}^2} = \frac{\pi^{1/2}\gamma^{3/2} e^{\epsilon^2/\gamma}}{4}\left[\mathrm{erf}\left(\frac{h_D + \epsilon}{\gamma^{1/2}}\right)\right]_0^{h_{0D}} \tag{26}$$

where erf denotes the error function.

5.1.1. *Injection scenario*

For an injection scenario $\gamma = 1$, and recalling Eq. (21), Eq. (26) reduces to

$$r_{eD} = \left[\frac{\pi^{1/2} e^{\epsilon^2} \text{erfc}(\epsilon)}{4t_D}\right]^{-1/2} \tag{27}$$

where erfc denotes the complementary error function.

A relevant expansion for erfc(x) includes (Wolfram Research, Inc., 2015)

$$\text{erfc}(x) = \frac{e^{-x^2}}{\pi^{1/2}}\left(\frac{1}{x} - \frac{1}{2x^3} + O(x^{-5})\right) \tag{28}$$

from which it follows that

$$r_{eD} = \left[\frac{1}{4t_D}\left(\frac{1}{\epsilon} + O(\epsilon^{-3})\right)\right]^{-1/2} \tag{29}$$

5.1.2. *Production scenario*

For a production scenario $\gamma = -1$, and recalling Eq. (21), Eq. (26) reduces to

$$r_{eD} = \left[\frac{\pi^{1/2} e^{-\epsilon^2} \text{erfi}(\epsilon)}{4t_D}\right]^{-1/2} \tag{30}$$

where erfi denotes the imaginary error function. Also note that $\text{erfi}(x) = -i\text{erf}(ix)$, $\text{erfi}(0) = 0$ and $\text{erfi}(-x) = -\text{erfi}(x)$.

Relevant expansion for erfi(x) includes (Wolfram Research, Inc., 2015)

$$\text{erfi}(x) = -i + \frac{e^{x^2}}{\pi^{1/2}}\left[\frac{1}{x} + \frac{1}{2x^3} + O(x^{-5})\right] \tag{31}$$

from which it follows that

$$r_{eD} = \left[\frac{1}{4t_D}\left(\frac{1}{\epsilon} + O(\epsilon^{-3})\right)\right]^{-1/2} \tag{32}$$

5.1.3. Correction for early-time response

For large ϵ, Eq. (24) reduces to

$$h_D = \frac{1}{\epsilon}\ln\left(\frac{r_{eD}}{r_D}\right), \quad \epsilon \gg 2h_D \tag{33}$$

Interestingly, for large times, Eq. (16) can be written as (Cooper and Jacob, 1946)

$$h_D = \frac{1}{\epsilon}\ln\left(\frac{r_{eD}e^{-0.5772/2}}{r_D}\right) \tag{34}$$

where r_{eD} is found from Eq. (29).

Furthermore, substitution of Eq. (29) into Eq. (16) leads to

$$h_D = \frac{1}{2\epsilon}E_1\left(\frac{r_D^2}{r_{eD}^2}\right) \tag{35}$$

By further consideration of Eq. (24), it therefore follows that a better approximation to the full Darcian problem of concern takes the form

$$h_D = \gamma E_1\left(\frac{r_D^2}{r_{eD}^2}\right)\left\{\epsilon + \left[\epsilon^2 + \gamma E_1\left(\frac{r_D^2}{r_{eD}^2}\right)\right]^{1/2}\right\}^{-1} \tag{36}$$

where r_{eD} is found from

$$r_{eD}^{-2} = \frac{\pi^{1/2} e^{\epsilon^2/\gamma}}{4t_D}\begin{cases} \text{erfc}(\epsilon), & \gamma = 1 \\ \text{erfi}(\epsilon), & \gamma = -1 \end{cases} \tag{37}$$

As ϵ becomes large, Eq. (36) converges exactly on to the Theis solution, given in Eq. (16), for both small and large times.

5.2. Approximate solution for large β

For very large β values, Eq. (15) should be replaced with

$$\gamma\beta q_D^2 = -\frac{\partial h_D}{\partial r_D} \tag{38}$$

which on substitution into Eq. (17) leads to

$$\frac{\gamma\beta}{[(h_D + \epsilon)r_D]^2} = -\frac{\partial h_D}{\partial r_D} \tag{39}$$

which integrates to obtain

$$\frac{h_D^3}{3} + \epsilon h_D^2 + \epsilon^2 h_D = \gamma\beta\left(\frac{1}{r_D} - \frac{1}{r_{eD}}\right) \tag{40}$$

where again, r_{eD} is defined as the radial distance at which $h_D = 0$.

The only real root of Eq. (40) takes the form

$$h_D = (\epsilon^3 + F)^{1/3} - \epsilon \tag{41}$$

where

$$F = 3\gamma\beta\left(\frac{1}{r_D} - \frac{1}{r_{eD}}\right) \tag{42}$$

To better understand how Eq. (41) behaves for large ϵ, it is useful to multiply the top and bottom by

$$(\epsilon^3 + F)^{2/3} + (\epsilon^3 + F)^{1/3}\epsilon + \epsilon^2 \tag{43}$$

which reveals that

$$h_D = \frac{F}{(\epsilon^3 + F)^{2/3} + (\epsilon^3 + F)^{1/3}\epsilon + \epsilon^2} \tag{44}$$

5.2.1. Zero ϵ scenario

When $\epsilon = 0$, Eq. (41) reduces to

$$h_D = \left[3\gamma\beta\left(\frac{1}{r_D} - \frac{1}{r_{eD}}\right)\right]^{1/3} \tag{45}$$

which can be rearranged to get

$$r_D^2 = \left(\frac{h_D^3}{3\gamma\beta} + \frac{1}{r_{eD}}\right)^{-2} \tag{46}$$

which on substitution into Eq. (20) leads to (Wolfram Research, Inc., 2015)

$$t_D = \left\{ \frac{\gamma r_{eD}^{5/3} \eta^{1/3}}{18} \left[\ln\left(\frac{(r_{eD}^{1/3} h_D + \eta^{1/3})^2}{r_{eD}^{2/3} h_D^2 - \eta^{1/3} r_{eD}^{1/3} h_D + \eta^{2/3}} \right) - 2(3^{1/2}) \arctan\left(\frac{1 - 2(r_{eD}/\eta)^{1/3} h_D}{3^{1/2}} \right) \right] + \frac{\gamma \eta r_{eD}^2 h_D}{6(r_{eD} h_D^3 + \eta)} \right\}_0^{h_{0D}} \tag{47}$$

where $\eta = 3\gamma\beta$.

Eq. (47) can be simplified substantially to obtain

$$r_{eD} = \begin{cases} \left[\frac{3^{13/2}}{\beta} \left(\frac{t_D}{2\pi} \right)^3 \right]^{1/5}, & \gamma = 1 \\ \infty, & \gamma = -1 \end{cases} \tag{48}$$

5.2.2. Large ϵ scenario

When $\epsilon \gg F$, Eq. (40) reduces to

$$h_D = \frac{\gamma\beta}{\epsilon^2} \left(\frac{1}{r_D} - \frac{1}{r_{eD}} \right) \tag{49}$$

which on substitution into Eq. (18) and rearranging leads to

$$r_{eD} = \frac{2\epsilon^2 t_D}{\beta} \tag{50}$$

5.2.3. Intermediate ϵ scenario

From the above sub-sections it can be seen that r_{eD} grows with t_D at different rates depending on ϵ. Eqs. (48) and (50) intersect when $t_D = t_{cD}$, where t_{cD} is a dimensionless critical time, found from

$$t_{cD} = \frac{3^{13/4}\beta^2}{16\pi^{3/2}\epsilon^5} \tag{51}$$

For intermediate values of ϵ, a good approximation for r_{eD} can be obtained from

$$r_{eD} = \begin{cases} \left[\dfrac{3^{13/2}}{\beta}\left(\dfrac{t_D}{2\pi}\right)^3\right]^{1/5} & t_D < t_{cD} \\ \\ \dfrac{2\epsilon^2 t_D}{\beta} & t_D \geq t_{cD} \end{cases} \tag{52}$$

6. Solution by matched asymptotic expansion

At large times, the head profile has spread out over a large distance. This can be specified by writing (Roose et al., 2001)

$$t_D = \frac{\epsilon^2\tau}{\beta^2} \quad \text{and} \quad r_D = \frac{\epsilon R}{\beta} \tag{53}$$

Let the outer and inner limit processes of h_D be denoted h_0 and h_0^*, respectively.

6.1. Solution for the outer limit process

The solution of the outer limit process takes the form (recall Eq. (16)) (Roose et al., 2001; Mathias et al., 2008)

$$h_0 = BE_1\left(\frac{R^2}{4\epsilon\tau}\right) \tag{54}$$

where B is an integration constant yet to be defined and E_1 denotes the exponential integral function.

6.2. *Solution for the inner limit process*

For the inner region near the injection well, it is better to revert back to the variable r_D such that the inner limit process is characterized by

$$\frac{\beta^2}{\epsilon^2}\frac{\partial h_0^*}{\partial \tau} = -\frac{1}{r_D}\frac{\partial}{\partial r_D}\left[r_D\left(h_0^* + \epsilon\right) q_0^*\right] \tag{55}$$

where

$$q_0^* + \beta |q_0^*| q_0^* = -\frac{\partial h_0^*}{\partial r_D} \tag{56}$$

from which it follows that

$$\frac{\partial}{\partial r_D}\left[r_D\left(h_0^* + \epsilon\right) q_0^*\right] = O\left(\frac{\beta^2}{\epsilon^2}\right) \tag{57}$$

Integrating Eq. (57) with respect to r_D and applying the $r_D \rightarrow 0$ boundary condition in Eq. (11) then leads to

$$q_0^* = \frac{\gamma}{\left(h_0^* + \epsilon\right) r_D} \tag{58}$$

which, on substitution into Eq. (56) yields

$$\frac{1}{\left(h_0^* + \epsilon\right) r_D} + \frac{\beta}{\left(h_0^* + \epsilon\right)^2 r_D^2} = -\frac{1}{\gamma}\frac{\partial h_0^*}{\partial r_D} \tag{59}$$

Following an approach previously adopted by Terzidis (2003) to look at steady state non-

198 Darcian radial flow in an unconfined aquifer, consider a reference point situated a dimensionless
199 radial distance away from the origin, r_{wD}. Let h^*_{w0} be the value of h^*_0 at $r_D = r_{wD}$. Substituting
200 $u = h^*_0 - h^*_{w0}/2$ into Eq. (59) leads to

$$\frac{\partial u}{\partial r_D} = -\frac{2\gamma}{\left(2u + h^*_{w0} + 2\epsilon\right) r_D}\left[1 + \frac{2\beta}{\left(2u + h^*_{w0} + 2\epsilon\right) r_D}\right] \tag{60}$$

201 Taking advantage of the expansion

$$(x + a)^{-1} = a^{-1} - xa^{-2} + x^2a^{-3} + O(a^{-4}) \tag{61}$$

202 it can be seen that

$$\frac{\partial u}{\partial r_D} = -\frac{2\gamma}{\left(2u + h^*_{w0} + 2\epsilon\right) r_D}\left[1 + \frac{2\beta}{\left(h^*_{w0} + 2\epsilon\right) r_D}\right] + O\left((h^*_{w0} + 2\epsilon)^{-3}\right) \tag{62}$$

203 Separating variables and integrating with respect to r_D yields

$$u^2 + (h^*_{w0} + 2\epsilon)u - 2G = 0 \tag{63}$$

204 where

$$G = \gamma\left[\frac{2\beta}{(h^*_{w0} + 2\epsilon)r_D} - \ln r_D\right] + C \tag{64}$$

205 The positive root of Eq. (63) is of practical interest:

$$2u = -(h_{w0}^* + 2\epsilon) + [(h_{w0}^* + 2\epsilon)^2 + 8G]^{1/2} \tag{65}$$

206 Taking advantage of the expansion

$$(x + a)^{1/2} = a^{1/2} + \frac{x}{2a^{1/2}} - \frac{x^2}{8a^{3/2}} + O(a^{-5/2}) \tag{66}$$

207 and reversing the u substitution it can be seen that

$$h_0^* = \frac{h_{w0}^*}{2} + \frac{2G}{(h_{w0}^* + 2\epsilon)} - \frac{4G^2}{(h_{w0}^* + 2\epsilon)^3} + O\left((h_{w0}^* + 2\epsilon)^{-5}\right) \tag{67}$$

208 Noting that the truncation error in Eq. (62) is $O\left((h_{w0}^* + 2\epsilon)^{-3}\right)$, for consistency, the third term

209 on the right-hand-side of Eq. (67) should also be excluded such that it can be said that

$$h_0^* = D + \gamma\left[\frac{4\beta}{(h_{w0}^* + 2\epsilon)^2 r_D} - \frac{2\ln r_D}{(h_{w0}^* + 2\epsilon)}\right] + O\left((h_{w0}^* + 2\epsilon)^{-3}\right) \tag{68}$$

210 where D is a constant found from

$$D = \frac{h_{w0}^*}{2} + \frac{2C}{(h_{w0}^* + 2\epsilon)} \tag{69}$$

211 *6.3. Matching of inner and outer limit processes*

212 The constants B and D are determined by matching the inner and outer limit processes, i.e.

$$\lim_{r_D \to \infty} h_0^* = \lim_{R \to 0} h_0 \tag{70}$$

213 Exploiting the asymptotic expansion of the E_1 function for small R, Eq. (54) can be written in
214 the from

$$h_0 = -B\left[0.5772 + 2\ln r_D + \ln\left(\frac{\beta^2}{4\epsilon^3\tau}\right)\right] + O\left(\left(\frac{\beta}{\epsilon}\right)^2\right) \tag{71}$$

215 Therefore, by comparing Eqs. (68) and (71), it can be seen that

$$B = \frac{\gamma}{h_{w0}^* + 2\epsilon} \tag{72}$$

$$D = -\frac{\gamma}{(h_{w0}^* + 2\epsilon)}\left[0.5772 + \ln\left(\frac{\beta^2}{4\epsilon^3\tau}\right)\right] + O\left(\left(\frac{\beta}{\epsilon}\right)^2\right) \tag{73}$$

216 Similar to Mathias et al. (2008), adding the inner and outer limits and subtracting out of their
217 sum the term that is common to both expressions in the overlap region then yields the composite
218 solution

$$h_D = \frac{\gamma}{(h_{wD} + 2\epsilon)}E_1\left(\frac{r_D^2}{4\epsilon t_D}\right) + \frac{4\gamma\beta}{(h_{wD} + 2\epsilon)^2 r_D} + O\left(\left(\frac{\beta}{\epsilon}\right)^2\right) \tag{74}$$

219 where $h_{wD} = h_D(r_D = r_{wD})$.

220 *6.4. Determining h_{wD}*

221 The h_{wD} term can be obtained by finding the real root of the cubic equation

$$(h_{wD} + 2\epsilon)^3 - 2\epsilon(h_{wD} + 2\epsilon)^2 - \gamma E_1\left(\frac{r_{wD}^2}{4\epsilon t_D}\right)(h_{wD} + 2\epsilon) - \frac{4\gamma\beta}{r_D} = 0 \tag{75}$$

which takes the form (Wolfram Research, Inc., 2015)

$$h_{wD} = \left[\left(T_1^2 - T_2^3\right)^{1/2} + T_1\right]^{1/3} + T_2\left[\left(T_1^2 - T_2^3\right)^{1/2} + T_1\right]^{-1/3} - \frac{4\epsilon}{3} \tag{76}$$

where

$$T_1 = \frac{8\epsilon^3}{27} + \frac{\gamma\epsilon}{3}E_1\left(\frac{r_{wD}^2}{r_{eD}^2}\right) + \frac{2\gamma\beta}{r_{wD}} \tag{77}$$

$$T_2 = \frac{4\epsilon^2}{9} + \frac{\gamma}{3}E_1\left(\frac{r_{wD}^2}{r_{eD}^2}\right) \tag{78}$$

$$r_{eD} = (4\epsilon t_D)^{1/2} \tag{79}$$

Furthermore, it can be understood that a better approximation for h_D is obtained from

$$h_D = h_{wD}(r_{wD} = r_D) \tag{80}$$

and the approximation becomes identical to Eq. (36) when $\epsilon = 0$ and $\beta = 0$ if r_{eD} is calculated from Eq. (37) instead. Readers may benefit from the identity

$$i^{\nu} + i^{-\nu} = 2\cos\left(\frac{\nu\pi}{2}\right) \tag{81}$$

when verifying this for themselves.

7. Comparison with a finite difference solution

The study reported in this article has led to the development of three different approximate solutions for production and injection wells in unconfined aquifers. The first approximate solution, Eqs. (36) to (37), reported in section 5.1, is hereafter referred to as the zero β quasi-steady-state (QSS) solution. The second approximate solution, Eqs. (44), (42), (51) and (52), reported in section 5.2, is hereafter referred to as the large β QSS solution. The third approximate solution, Eq. (80), Eqs. (76) to (78) and Eq. (37), reported in section 6.0, is hereafter referred to as the matched asymptotic expansion solution.

To demonstrate the accuracy of the approximate solutions described above, results from the approximate solutions are compared to equivalent results from a finite difference solution for the full problem described in section 3.

The finite difference solution is obtained in exactly the same way as previously presented by Mathias et al. (2008) but with the addition of the $(h_D + \epsilon)$ factor on the q_D values shown in Eq. (8), specifically associated with unconfined aquifers. To summarize, the partial differential equation in section 3 is discretised in space using finite differences. The resulting set of non-linear ordinary differential equations (ODE) with respect to time are then integrated collectively using MATLAB's stiff ODE solver, ODE15s. The dimensionless radial distance, r_D, is discretised into 100 logarithmically spaced points, with the space steps ranging across four orders of magnitude, with the smallest space steps around the injection/production well. The $r_D \rightarrow 0$ and $r_D \rightarrow \infty$ boundary conditions are approximated by instead applying the associated boundary conditions at $r_D = 0.1$ and $r_D = 1000$, respectively. Manual specification of a time-step is not required because

ODE15s adaptively chooses time-steps as the solution progresses.

An appropriate range of ϵ and β values to be studied were determined as follows. In a recent set of packed column experiments, Salahi et al. (2015) determined A [$L^{-1}T$] and B [$L^{-2}T^2$] coefficients for the Forchheimer equation in the form

$$Aq + Bq|q| = -\frac{\partial h}{\partial r} \tag{82}$$

for a wide range of of rounded and crushed granular materials. By simple inspection it can be seen that $K = A^{-1}$ and $\beta = B/A^2$. From their Table 1, it can therefore be shown that Salahi et al. (2015) observed K values ranging from 0.022 ms^{-1} to 0.940 ms^{-1} and β values ranging from 1.438 to 153.7.

Possible production and injection rates can be expected to range from 0.01 to 10.0 Ml/day whereas h_i might range from 1 m to 100 m. Considering that

$$\epsilon = \left(\frac{2\pi K h_i^2}{Q_0}\right)^{1/2} \tag{83}$$

it therefore also follows that practical values for ϵ range from 1.1 to 23,000.

Fig. 1 shows plots of dimensionless pressure against dimensionless distance for a range of dimensionless times for the special case when $\beta = 0$ for an injection scenario (i.e., $\gamma = 1$). The first thing to note is that the matched asymptotic expansion solution and the zero β QSS solution produce identical results for all ϵ. The numerical model also produces almost identical results for $\epsilon \geq 1$. When $\epsilon = 0$ the finite difference model has less hydraulic head dispersion around the radius of influence (i.e., where h_D approaches zero). It is also interesting to see how hydraulic

head distance profiles deviate from a linear-log relationship, normally associated with the Theis solution, when $\epsilon < 10$.

Fig. 2 shows plots of dimensionless pressure against dimensionless distance for a range of dimensionless times for the case when $\beta = 100$ again for an injection scenario (i.e., $\gamma = 1$). The close correspondence between the large β QSS solution for $\epsilon \leq 1$ helps confirm that the finite difference solution is performing in an accurate fashion for these scenarios. The divergence between the finite difference solution and the QSS solution for larger values of ϵ comes about because the Darcian component (which is ignored in the large β QSS solution) becomes more important when ϵ is larger. The matched asymptotic expansion solution is less effective at describing these scenarios except for when $\epsilon \geq 100$ and $t_D \geq 100$ when $\epsilon = 10$. This discrepancy is consistent with the order of accuracy assumed when deriving the matched asymptotic expansion solution. Furthermore, it shows that the non-Darcy component of the Forchheimer equation is more important for small ϵ values (i.e., aquifers with a stronger unconfined, as opposed to confined, response).

Fig. 3 shows plots of dimensionless pressure against dimensionless distance for a range of dimensionless times for a production scenario (i.e., $\gamma = -1$) when $\beta = 0$ and $\beta = 1$. Note that it is not possible to solve this problem for $\epsilon = 0$ because this would imply that there is no water to produce. Figs. 3 a) and b) show production cases for when $\beta = 0$. Here it can be seen that there is excellent correspondence between the finite difference solution, the matched asymptotic expansion solution and the zero β QSS solution. Note that the solution for $\epsilon = 3$ was only simulated up to $t_D = 10$ because shortly after that the well dries out.

Figs. 3 c) and d) show results for water production with the Forchheimer equation (with $\beta = 1$). It is difficult to look at production scenarios with β much greater than one in conjunction with

moderate values of ϵ (i.e., $\epsilon \leq 10$), because the production well dries out too fast. Consequently the large β QSS solution is not useful in this context. Furthermore, it can be understood that it is difficult to study the significance of Forchheimer flow under strongly unconfined conditions for the production scenario, because the Dupuit assumption quickly becomes invalid in the region of interest. Nevertheless, it can be seen that the matched asymptotic expansion solution is capable of accurately predicting the results from the finite difference solution for these scenarios.

By comparing Figs. 3 b) (where $\epsilon = 10$ and $\beta = 0$) to Fig. 3 d) (where $\epsilon = 10$ and $\beta = 1$), it can be seen that in the latter case, where the inertial effects are non-negligible, the drawdown is more significant in the well vicinity. For example for $t_D = 100$, $r_D = 0.1$ and for $\beta = 0$, $h_D = -0.64$ whereas for the same case but with $\beta = 1$, $h_D = -0.75$. However, for larger distances, where the velocities are smaller and subsequently the inertial effects become negligible, the values of the heads become identical for both values of β, because flow is Darcian in this region.

8. Summary and conclusions

This article presents a series of approximate solutions to look at Forchheimer flow around a production well and injection well in an unconfined aquifer. All the presented solutions invoke the Dupuit assumption that vertical flow is negligible.

The first approximate solution involved imposing a quasi-steady-state assumption and fixing $\beta = 0$ (and hence solves for Darcy's law only). The quasi-steady-state assumption allows the treatment of the hydraulic head distribution around the injection/production well as a steady state profile with a radius of influence, which moves out with increasing time. The location of the radius of influence is determined by forcing the integral of the hydraulic head distribution with respect

311 to distance to be consistent with the volume of water that has been injected or produced at that
312 particular point in time.

313 The second approximate solution involved imposing the same quasi-steady-state assumption
314 but with β assumed to be sufficiently large such that the Darcy component of the Forchheimer
315 equation can be ignored. This large β solution is particularly applicable for coarse grained aquifers,
316 where small water table gradients (consistent with the Dupuit assumption) often coincide with
317 fully developed turbulent conditions (consider the discussion in Moutsopoulos, 2009, Appendix
318 A).

319 The third approximate solution was obtained by solving the full problem using the method
320 of matched asymptotic expansions. The latter solution is valid for $O\left((\beta/\epsilon)^2\right)$. For large values
321 of β, large head losses occur. For small values of ϵ, either the initial water table height is small
322 or the pumping rate is large so that again the associated head losses are expected to be large.
323 Interestingly, for large values of the ratio, β/ϵ, for the production well case, the well is predicted
324 to quickly dry out such that the Dupuit assumption does not hold.

325 The three approximate solutions were compared to results from a finite difference solution
326 modified from the finite difference solution previously presented by Mathias et al. (2008) for con-
327 fined aquifers. The quasi-steady-state solutions were able to verify the finite difference solution
328 when $\beta = 0$ and when $\beta = 100$ is very large whilst $\epsilon \leq 10$. The matched asymptotic expansion
329 solution was found to accurately predict the finite difference results providing the ratio of β/ϵ is
330 suitably small. The results also illustrate that the non-Darcy component of the Forchheimer equa-
331 tion is more important for small ϵ values (i.e., aquifers with a stronger unconfined, as opposed to
332 confined, response).

Overall, the analysis has added further support to the idea that non-Darcy effects are likely to be important around both injection wells and production wells in unconfined aquifers. The matched asymptotic expansion solution derived was found to be accurate for most of the practical cases studied. The solution is simple to evaluate and should be considered for future numerical modeling studies as an important model verification tool.

9. References

Babu, D. K. and van Genuchten, M. T. (1980), A perturbation solution of the nonlinear Boussinesq equation: the case of constant injection into a radial aquifer, Journal of Hydrology, 48, 269–280.

Barenblatt, G. I., Entov, V. M.,Ryzhik, V. M. (1990), Theory of fluid flows through natural rocks, Kluwer, Dordrecht pp. 395.

Bear, J. (1979), Hydraulics of Groundwater, Mc-Graw-Hill, New York, 567 pp.

Bordier, C., and Zimmer, D. (2000), Drainage equations and non-Darcian modelling in coarse porous media or geosynthetic materials, Journal of Hydrology, 228, 174–187.

Bouwer, H. (2002), Artificial recharge of groundwater: hydrogeology and engineering, Hydrogeology Journal, 10, 121–142.

Cooper, H. H., and C. E. Jacob (1946), A generalized graphical method for evaluating formation constants and summarizing well field history, Trans. Amer. Geophys. Union, 27, 526–534.

Dillon, P. (2005), Future management of aquifer recharge, Hydrogeology Journal, 13, 313–316.

Donovan, D. J., Katzer, T., Brothers, K., Cole, E. and Johnson, M. (2002), Cost-benefit analysis of artificial recharge in Las Vegas Valley, Nevada, Journal of Water Resources Planning and Management, 128, 356–365.

Forchheimer, P. (1901), Wasserbewegung durch Boden, Z. Ver. Deutsch. Ing., 45, 1782–1788.

Hunt, B. W. (1971), Vertical recharge of unconfined aquifer, Journal of the Hydraulics Division, 97, 1017–1030.

Khan, S., Mushtaq, S., Hanjra, M. A. and Schaeffer, J. (2008), Estimating potential costs and gains from an aquifer storage and recovery program in Australia, Agricultural Water Management, 95, 477–488.

Li, L., Lockington, D. A., Parlange, M. B., Stagnitti, F., Jeng, D. S., Selker, J. S., Telyakovskiy, A. S., Barry D. E., Parlange, J. Y. (2005), Similarity solution of axisymmetric flow in porous media, Advances in Water Resources, 28, 1076–1082.

Manglik, A., Rai, S. N. and Singh, R. N. (1997), Response of an unconfined aquifer induced by time varying recharge from a rectangular basin, Water Resources Management, 11, 185–196.

Marino, M. A., and Yeh, W. W. (1972), Nonsteady flow in a recharge well-unconfined aquifer system, Journal of Hydrology, 16, 159–176.

Mathias, S. A., A. P. Butler, and H. Zhan (2008), Approximate solutions for Forchheimer flow to a well, J. Hydraul. Eng., 134(9), 1318–1325.

Mathias, S. A., and Todman, L. C. (2010), Step-drawdown tests and the Forchheimer equation, Water Resour. Res., 46, W07514.

Mathias, S. A., McElwaine, J. N. and Gluyas, J. G. (2014), Heat transport and pressure buildup during carbon dioxide injection into depleted gas reservoirs, Journal of Fluide Mechanics, 756, 89–109.

Mathias, S. A. and Wen, Z. (2015), Numerical simulation of Forchheimer flow to a partially penetrating well with a mixed-type boundary condition, Journal of Hydrology, 524, 53–61.

Moutsopoulos K. N. (2007), One-dimensional unsteady inertial flow in phreatic aquifers, induced by a sudden change of the boundary head, Transport in Porous Media, 70, 97–125.

Moutsopoulos K. N. (2009), Exact and approximate analytical solutions for unsteady fully developed turbulent flow in porous media and fractures for time dependent boundary conditions, Journal of Hydrology, 369, 78–89.

Moutsopoulos K. N., Papaspyros, J. N. E. and Tsihrintzis, V. A. (2009), Experimental investigation of inertial flow processes in porous media, Journal of Hydrology, 374, 242–254.

Pliakas, F., Petalas, C., Diamantis, I. and Kallioras, A. (2005), Modeling of groundwater artificial recharge by reactivating an old stream bed, Water Resources Management, 19, 279–294.

Rai, S. N. and Singh, R. N. (1995), Two-dimensional modelling of water table fluctuation in response to localised transient recharge, Journal of Hydrology, 167, 167–174.

Rai, S. N., Ramana, D. V., and Singh, R. N. (1998), On the prediction of ground-water mound formation in response

to transient recharge from a circular basin, Water Resources Management, 12, 271–284.

Roose, T., Fowler, A. C., and Darrah, P. R. (2001), A mathematical model of plant nutrient uptake, Journal of Mathematical Biology, 42, 347–360.

Rygaard, M., Binning, P. J., and Albrechtsen, H. J. (2011), Increasing urban water self-sufficiency: New era, new challenges, Journal of Environmental Management, 92, 185–194.

Salahi, M. B., Sedgh-Asl, M., and Parvizi, M. (2015), Nonlinear flow through a packed-column experiment, ASCE Journal of Hydrological Engineering, DOI:10.1061/(ASCE)HE.1943-5584.0001166.

Sen, Z. (1986), Volumetric approach to non-Darcy flow in confined aquifers, Journal of Hydrology, 87, 337–350.

Sheng, Z. (2005), An aquifer storage and recovery system with reclaimed wastewater to preserve native groundwater resources in El Paso, Texas, Journal of Environmental Management, 75, 367–377.

Teloglou I., Zissis, T. S. and Panagopoulos, C. A. (2008), Water table fluctuation in aquifers overlying a semi-impervious layer due to transient recharge from a circular basin, Journal of Hydrology, 348, 215–223.

Terzidis G. (2003), Steady non-Darcian groundwater flow in unconfined aquifers, 9th Conference of the Greek Hydrotechnical Association pp. 369-376, Thessaloniki, Greece, 2nd -5th April 2003. In Greek.

Theis, C. V. (1935), The relationship between the lowering of the piezometric surface and the rate and duration of discharge of a well using ground water storage, Trans. Amer. Geophys. Union, 16, 519–524.

Wolfram Research, Inc. (2015), Wolfram Alpha, Wolfram Research, Inc., Champaign, Illinois.

Yeh, H. D. and Chang, Y. C. (2013), Recent advances in modeling of well hydraulics, Advances in Water Resources, 51, 27–51.

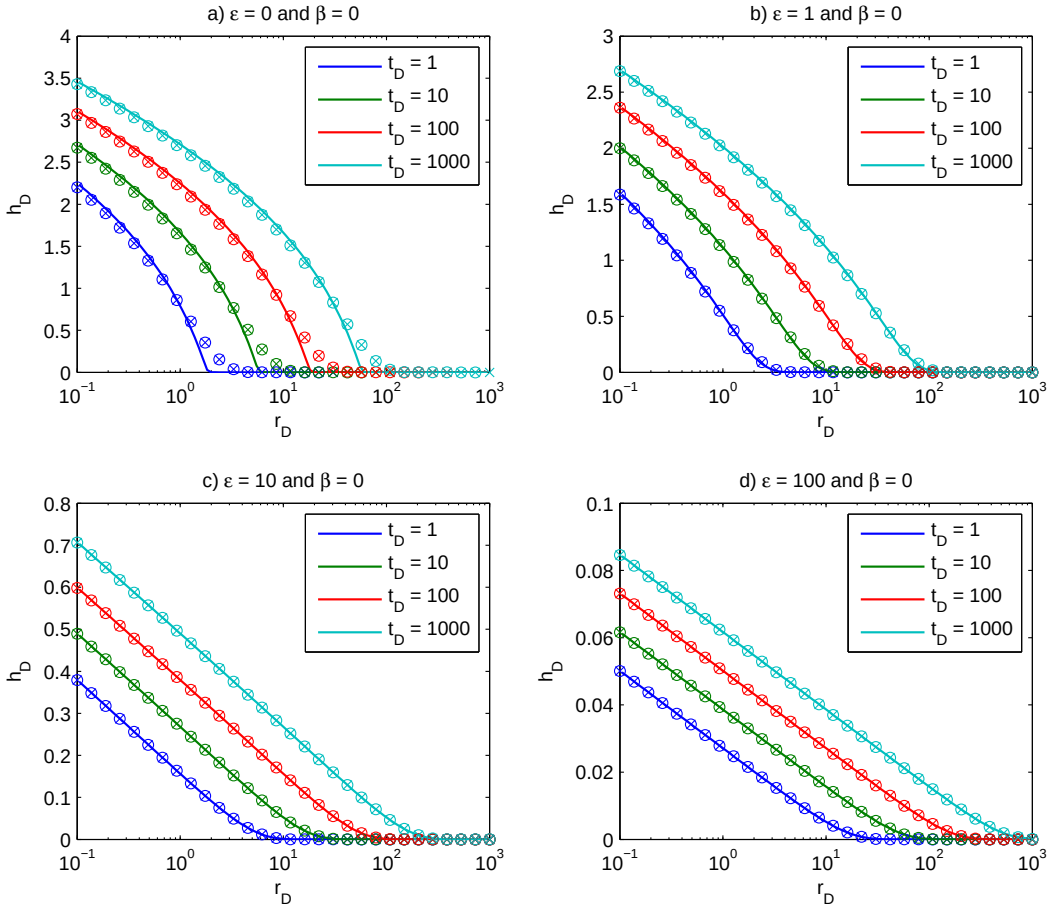

Figure 1: Plots of dimensionless hydraulic head, h_D, against dimensionless distance from an injection well (i.e. with $\gamma = 1$), r_D, for dimensionless times, t_D, as indicated in the legends. The values of ϵ and β applied are indicated in the subplot titles. The solid lines are from the finite difference solution of the full problem. The circular markers are from the matched asymptotic expansion solution. The cross markers are from the zero β quasi-steady-state solution.

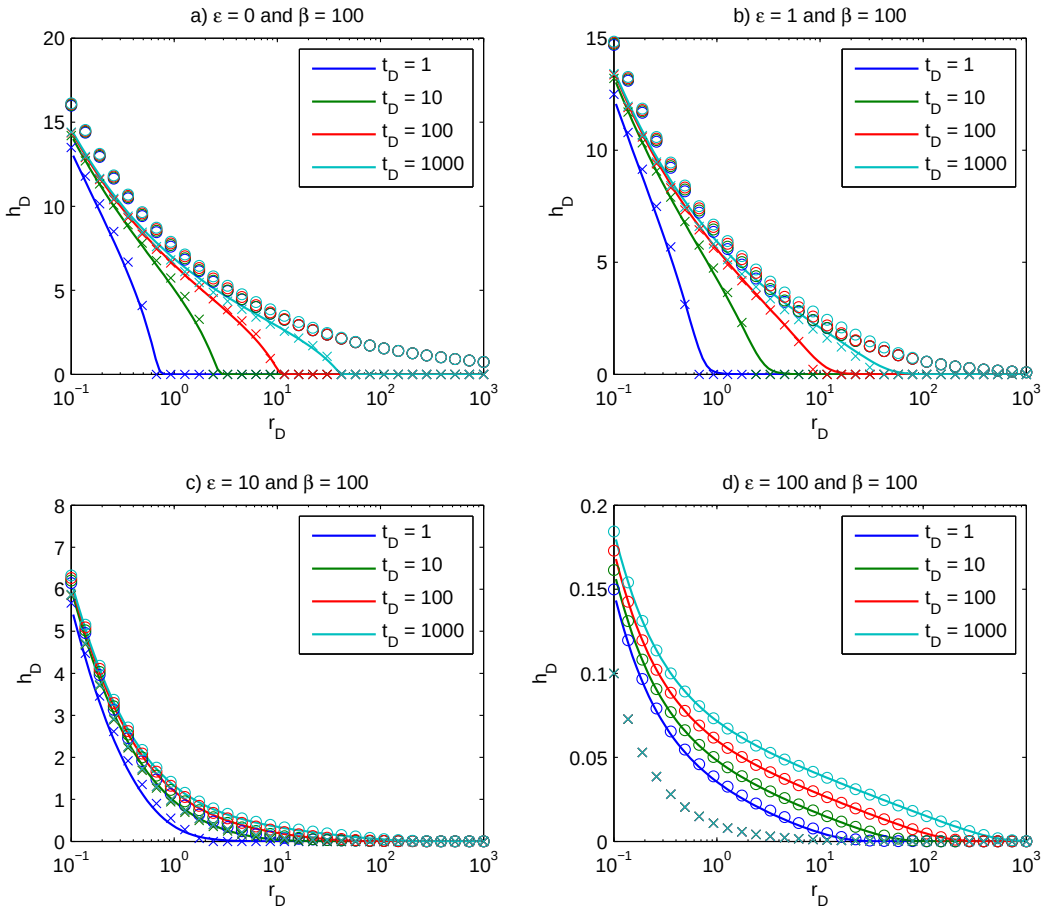

Figure 2: Plots of dimensionless hydraulic head, h_D, against dimensionless distance from an injection well (i.e. with $\gamma = 1$), r_D, for dimensionless times, t_D, as indicated in the legends. The values of ϵ and β applied are indicated in the subplot titles. The solid lines are from the finite difference solution of the full problem. The circular markers are from the matched asymptotic expansion solution. The cross markers are from the large β quasi-steady-state solution.

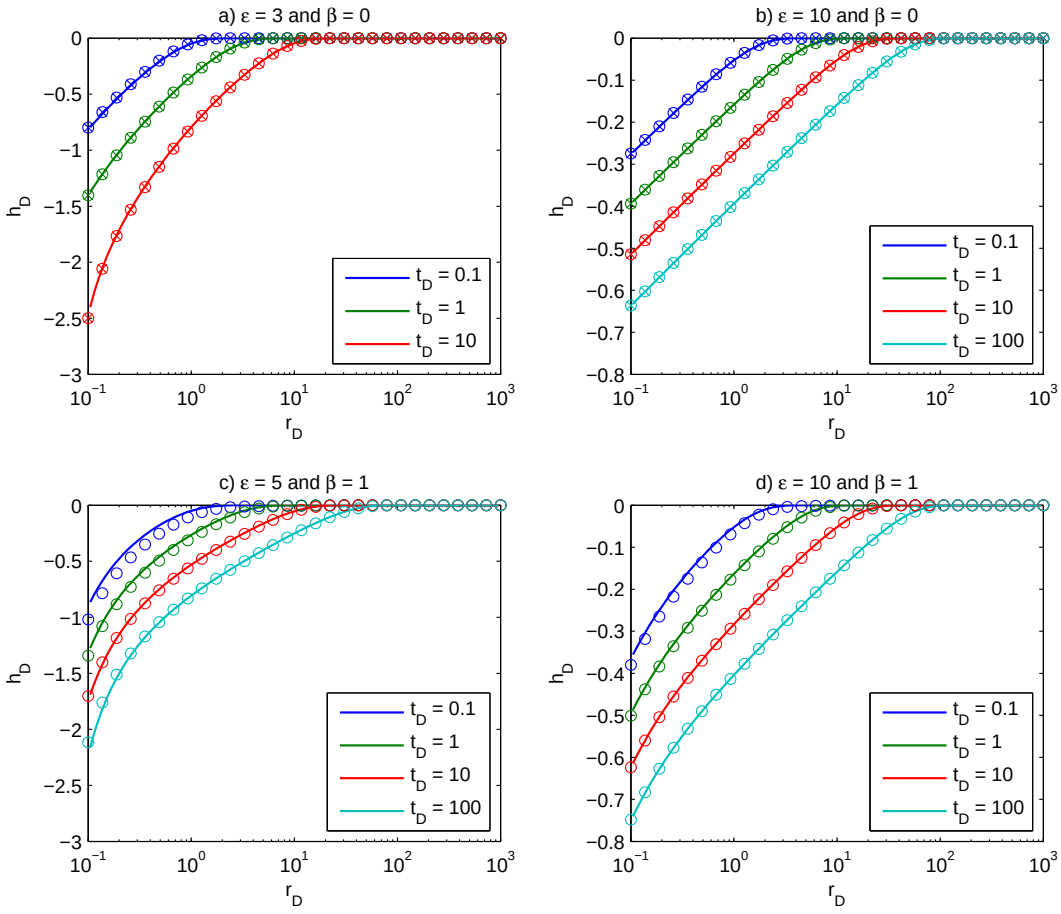

Figure 3: Plots of dimensionless hydraulic head, h_D, against dimensionless distance from a production well (i.e. with $\gamma = -1$), r_D, for dimensionless times, t_D, as indicated in the legends. The values of ϵ and β applied are indicated in the subplot titles. The solid lines are from the finite difference solution of the full problem. The circular markers are from the matched asymptotic solution. The cross markers are from the zero β quasi-steady-state solution.